LIBS Analysis of Optical Surfaces and Thin Films

Christoph Gerhard, Jörg Hermann

LIBS Analysis of Optical Surfaces and Thin Films

Christoph Gerhard[1] and Jörg Hermann[2]

[1]University of Applied Sciences and Arts, Faculty of Engineering and Health, 37085 Göttingen, Germany
[2]Aix-Marseille University, CNRS, LP3, 13288 Marseille, France

Abstract

Elemental analyses of thin films and optical surfaces with complex compositions are challenging as the standard analytical techniques based on measurement calibration are difficult to apply. In this chapter, we show that calibration-free laser-induced breakdown spectroscopy presents a powerful solution, enabling rapid quantitative analyses of multi-elemental thin films or tiny surface volumes of optical materials with high analytical performances. Examples are given for classically polished optical glass and a nickel-chromium-molybdenum alloy film of 150 nm thickness. Thus, broadband spectra, recorded under experimental conditions that enable simple and accurate modeling of plasma emission, are processed via a calibration-free approach based on the calculation of the spectral radiance of a plasma in local thermodynamic equilibrium to deduce the elemental composition. The validation via energy-dispersive X-ray spectroscopy, inductively coupled plasma atomic emission spectroscopy, and Rutherford backscattering spectrometry illustrates that calibration-free LIBS is not only a promising tool, but already a reliable analytical technique.

1. Introduction

Glass is one of the oldest synthetic materials produced and used by mankind for millennia. The first instruction for the production of glass is a more than 2,600 years old cuneiform inscription that was found in the library of the ancient Assyrian king Ashurbanipal. It roughly says: "*Take 60 parts of sand, 180 parts of ash from sea plants, and 5 parts of chalk and you obtain glass.*" Even though this basic recipe is still valid for simple glass vessels or panes, modern technical and optical glasses feature a much more complex composition. For instance, special crown or flint glasses used for the manufacturing of optical components and systems partially feature more than 20 different elements that act as glass network formers, modifiers and stabilizers. Moreover, optically active surfaces are usually coated with different functional coatings such as mirrors, anti-reflection layers or polarizing thin films. Most of such coatings consist of dielectric compounds as for example magnesium fluoride, zinc sulfide or titanium dioxide and may contain further metallic components. Besides optical coatings, thin films are widely used in modern surface technology, for example as functional layers in tribology or passivation. Here, a huge variety of different compositions is in hand. The quantitative analysis of thin films and optical surfaces is thus a challenging task.

Here, quite different approaches and methods can be used [jem02,tre13]. The most common technique for glass analysis is X-ray Fluorescence (XRF) where the sample surface is excited by polychromatic X-ray irradiation. The resulting fluorescence signal emitted by recombination of electrons is then detected and evaluated. This approach allows the analysis of major, minor and trace elements. It is thus widely used in archeology [tan09,liu12,hod19] and forensic investigations [koo91,tre13]. However, elements with atomic numbers smaller than 5, as for example hydrogen, cannot be detected.

Another standard method for glass analysis is Inductively Coupled Plasma Atomic Emission Spectroscopy (ICP-AES). Here, the sample material is dissolved in acid, vaporized and then transported within an argon flux into an inductively coupled plasma for electronic excitation at a temperature of about 10,000 K. The sample atoms are thus ionized and excited, and consequently emit characteristic radiation. The spectrum obtained in that way is finally analyzed. Even though this approach enables

precise and quantitative analysis of solids as for example glasses [koz92], it is difficult to apply to thin films or to in-depth measurements of near-surface layers since for both applications, material with well-defined thickness needs to be dissolved by the used acid. However, ICP-AES is suitable for the detection of impurities within glasses or polishing re-deposition layers [nea05,nea09] where the limit of detection amounts to a few ppm, depending on the particular element [ger21]. As an alternative to sample vaporization via acid digestion, direct vaporization is possible via laser ablation. This process, laser ablation inductively coupled plasma optical emission spectrometry (LA-ICP-OES), has turned out to be a promising alternative elemental analysis technique for forensic applications [sch12].

The ions generated by inductively coupled plasmas can also be evaluated via inductively Coupled Plasma Mass Spectrometry (ICP-MS) where the determination of the sample composition is carried out on the basis of the ion mass and not the emitted radiation. Since this approach is well suited for the detection and quantification of traces of lowest concentration, it is applied for forensic investigations of glasses [duc02].

A further powerful analytical method based on the detection of ions is Secondary Ion Mass Spectroscopy (SIMS) [ben75]. Here, secondary ions are extracted from the sample surface by an incident beam of primary ions of heavy elements such as cesium. The evaluation of secondary ions is then performed by detecting either the mass-over-charge ratio m/q or the time of flight. In the latter case, the method is referred to as Time-of-Flight Secondary Ion Mass Spectroscopy (ToF-SIMS). SIMS is a versatile and powerful analytical technique that – if properly calibrated – is also capable of detecting and quantifying lowest impurities in both natural and synthetic glasses [mar14,reg16] as well as thin films [hat97]. A noteworthy important advantage of SIMS is the possibility of direct detection of hydrogen in glasses [yur89,ger12]. A further advantage – probably the most important one – is the fact that due to the measurement principle, depth-resolved measurements with high resolution can be performed.

Another common surface analysis technique based on the application of incident ions is Rutherford Backscattering Spectrometry (RBS). Here, the sample surface is irradiated by ions of low mass as for example hydrogen or helium, but high kinetic energy. Some of these ions are backscattered by the sample. The energy of such backscattered ions depends on several parameters, including the mass of the sample atom where scattering occurred. Hence, the sample composition can be determined by detecting the energy of backscattered ions. Since this energy also follows from the stopping power within the sample material, RBS enables depth-resolved measurements [per87] where the depth resolution is 2 to 10 nm, depending on the atomic mass of the elements within the sample, and the information depth amounts to some microns. It is thus a nondestructive technique for the depth-resolved analysis of the composition of coatings and thin films [jey12].

A further method for glass and thin film analysis is X-ray Photoelectron Spectroscopy (XPS), a well-established and widespread standard technique. This method is based on the external photoelectric effect. The sample surface is irradiated by X-rays where the Al-K_α line is frequently used. As a result of such irradiation, electrons are extracted from the outermost layer of the surface; the information depth of XPS amounts to about 10 nm. The sample composition is then obtained from the analysis of the number and binding energy of the detected electrons. Moreover, the detected signal does not only enable the measurement of the elemental composition, but also characterizes the binding states or bond types within the sample material. For instance, this allows the analysis of the oxidation states of glass oxides [jie90] or the structure of glasses and glass modifications [ony93,hol01,ban17]. This method is also very suitable for compositional measurements of coatings [ran18] and interfaces [hau93]. Even though XPS – and the related Auger electron spectroscopy (AES) – suffer from matrix effects [jab88,tan03] due to scattering of electrons within the sample material, it is one of the most accurate and powerful analytical tool for surface analysis.

Another widespread method, Energy Dispersive X-ray Spectroscopy (EDX, EDS), could be referred to as “inverse XPS”: an electron beam irradiates the sample surface and the resulting X-ray emission spectrum is analyzed. The advantage of this approach is the high spatial resolution since EDX-apparatuses are usually integrated in scanning electron microscopes (SEM). Thus, precise elemental mapping can be realized [dal10]. Even though this technique is suitable for the quantification of major

elements in glasses, its low sensitivity prevents the quantitative determination of traces and minor elements [fal06]. Moreover, surface charging may lead to severe overestimation of oxygen due to electron-beam induced oxidation on the one hand [ric96], and outgassing of oxygen from deeper regions caused by electron bombardment on the other hand [lin63].
Finally, the elemental composition of thin films and glasses can be determined via Laser-Induced Breakdown Spectroscopy (LIBS) – one of the oldest laser applications [bau13]. LIBS has turned out to be a suitable tool for thin film analysis [can05,owe10,in13,her19] and the determination of the chemical composition of glasses [ger14]. In both cases, accurate analysis of traces and impurities that may severely affect the functionality of coatings or glass surfaces is of specific interest. For instance, even lowest residues from operating materials used in optics manufacturing notably alter the index of refraction of polished glass surfaces [ger17b,ger21]. It was demonstrated that appropriate calibration, for example by using a multiple-step calibration procedure as reported by *Negre* and co-workers [neg15], might increase the measurement accuracy for such minor elements. However, merely calibration-free approaches enable accurate analyses of optics surfaces and thin films as presented hereafter.

2. Sensitivity-improved calibration-free LIBS

Generally, the accuracy of any quantitative analytical method strongly depends on precise calibration using appropriate standards with well-known and well-defined chemical composition. Moreover, the chemical composition of the standards used for calibration should be as close to the chemical composition of the samples to be measured as possible. This issue can be overcome by using calibration-free LIBS (CF-LIBS), as first suggested by Ciucci and co-workers in [ciu99]. Since then, this basic approach was successively refined [fu19] and CF-LIBS was used for thin film analysis by various authors [wid10,dav17]. Here, the analysis was based on the modeling of the emission spectrum of the laser-induced plasma [ciu99]. However, it turned out that the simple approaches used, where for example the plasma is assumed to be homogenous and uniform in terms of temperature and electron energy distribution and the effect of self-absorption is not considered, suffer from low accuracy [bul02]. These techniques are furthermore merely applicable to samples of simple composition, containing only a few elements.
Higher accuracy can be obtained when correcting for self-absorption [axe14] and improved analysis is obtained when realizing experimental conditions generating a plume that can be well described by the simple model of a uniform plasma in local thermodynamic equilibrium (LTE) as described in [her14] and [her17]. For such a plasma, the relevant data electron density n_e, plasma temperature T, concentration of an element C_x, and plasma dimension L can be derived from measuring the spectral radiance of the uniform plasma as described in detail in [ger14]. Here, the computed spectrum is iteratively approximated to the actually measured spectrum. This method is described in more detail in Chapter 5 of the present book. It has turned out to be a promising technique for quantitative elemental analysis of complex bulk materials, and especially optical glasses, where its analytical performance is comparable to the accuracy obtained with standard techniques [ger14].
The sensitivity can even be increased by further expansion of the measurement routine as presented in [che18]. This approach, sensitivity-improved calibration-free LIBS (SENSI-CF-LIBS), consists of a two-step procedure where two spectra with different time delays between the incident laser pulse and the detector gate are recorded as shown schematically in Figure 1. Major and minor elements are then quantified by the evaluation of the spectrum taken at the early time. Here, full LTE conditions are existent and Boltzmann equilibrium distributions of all plasma species are ensured by the large electron density. The analysis of a spectrum taken in partial LTE conditions at a later time further allows for the quantification of trace elements. This becomes possible since the continuum emission intensity is considerably lower in partial LTE. Low-intensity emission lines are thus observable with an improved signal-to-noise ratio.

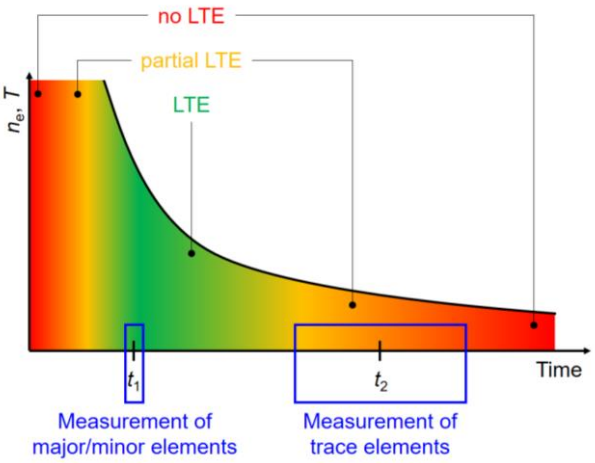

Figure 1. Time scheme for sensitivity-improved calibration-free LIBS based on the measurement of two spectra at different times. Major and minor elements are quantified in conditions of full LTE at an early time, t_1, whereas the concentration of trace elements is derived from the plasma in partial LTE at a later time, t_2.(Adapted from [che18])

Such Sensitivity-Improved Calibration-Free LIBS allows for the quantification of trace elements and impurities in the range of merely some ppm. As described above, this is achieved by fitting the computed spectral radiance to the actually measured spectrum as illustrated in Figure 2 for spectral lines used for minor and trace element analyses in seafood [che18].

The possibility of calibration-free quantification of trace elements without any extensive sample cleaning or preparation offers a number of new fields of applications and analytical tasks for LIBS. An emerging field is the investigation of glasses where the impact of manufacturing steps on the chemical composition of optics surfaces is of specific interest. Here, the approach of sensitivity-enhanced calibration-free LIBS is a promising technique for gaining further insight and knowledge about the interaction of glasses with ambient media.

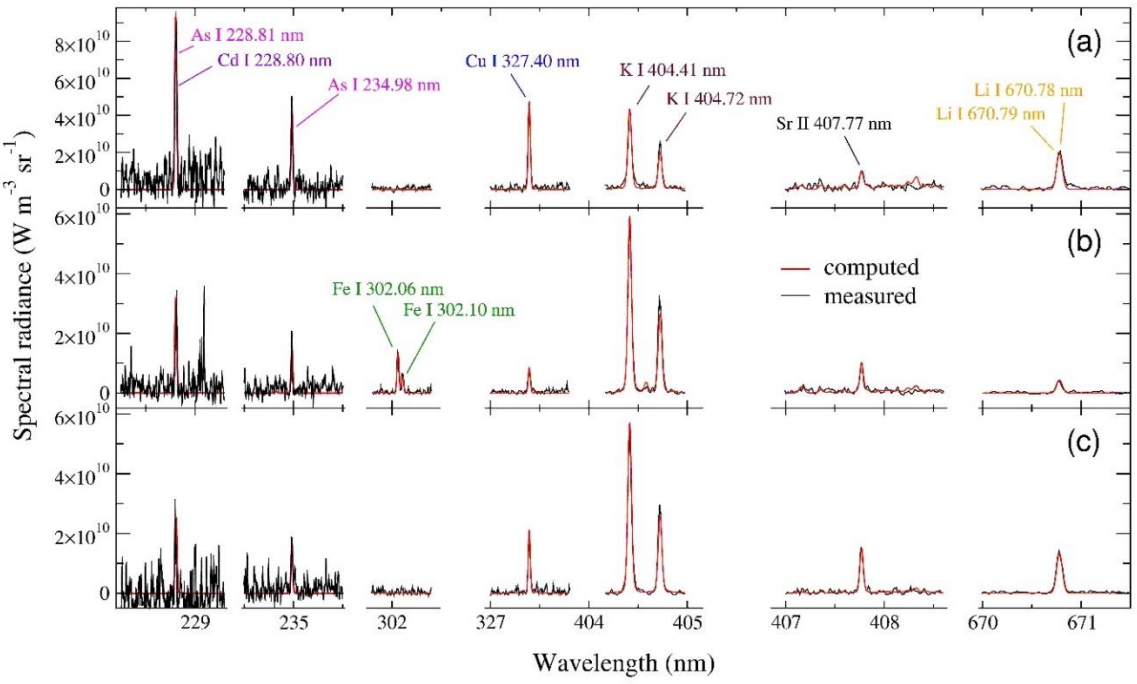

Figure 2. Computed and measured spectra for minor and trace element analysis in seafood [sepia (a), sardine (b), and octopus (c)] using sensitivity-improved calibration-free LIBS. (Adapted from [che18])

3. Analysis of optical materials and surfaces

3.1 Depth-resolved analysis of impurities

Optical components as for example lenses or prisms are usually manufactured by classical grinding, lapping and polishing [ger17]. The glass surface is thus in direct contact with different tools and operating materials in the course of the entire process. This leads to a certain contamination of the glass surface with traces from the manufacturing process, including for example wear debris from tools [lam02] or residues from polishing agents [nea05,sur15,ger17a]. Since such contaminants feature a gradual depth distribution [ger17b], a certain depth resolution is required for the investigation of manufacturing-induced impurities.

Depth-resolved analysis of surfaces can be realized by different methods or techniques presented in the Introduction. Applying XRF, a certain depth resolution can principally be achieved by confocal X-ray technology as recently reported [sun15]. However, obtaining depth-selective X-ray spectra is a challenging task [kan12] and the resolution is quite limited to the range of some tens of microns [nak09].

A very high depth resolution of generally a few nanometers [cha08] can be achieved by SIMS. This is due to its functional principle, the removal of thin layers from the sample surface by ion beam sputtering for signal generation [ben75]. Depending on the dose of ion irradiation, even depth resolutions in the range of some angstroms can be achieved [mah17]. It should however be noted that the incident ion beam might falsify the measurement results since the measured concentration depends on the etch rate of ions [kaa18].

The effect of surface sputtering is also used in some XPS-apparatuses where usually argon ion guns are applied for the removal of thin layers. The alternating layer removal and actual XPS measurement of the freshly generated surface allows for in-depth measurements where the resolution depends on sputter time. For instance, the sputter rate on fused silica is about 2 nm/minute for standard settings. However, as also valid for SIMS, ion implantation that occurs during sputtering potentially gives rise to a change in chemical composition [yam11] and may thus falsify the measurement results for deeper regions. This also applies to uncertainties caused by selective and thus non-stoichiometric sputtering [ekt00]. A certain depth resolution can thus also be realized without any sputtering, but by varying the angle of incidence of the exciting X-ray beam. This approach can also be applied for EDS analyses where, however, the penetration depth is generally significantly higher than for XPS.

An – as a manner of speaking – indirect approach is the HF etching of thin glass layers with defined thickness and the subsequent analysis of the etched-off material, for example using ICP-AES [nea05,nea09]. This approach requires high carefulness in order to avoid a contamination of the gained sample material. The depth resolution depends on etching time but is generally lower than for SIMS and argon gun-assisted XPS. However, for a number of applications, such high resolution as achievable by ion sputtering techniques is not required.

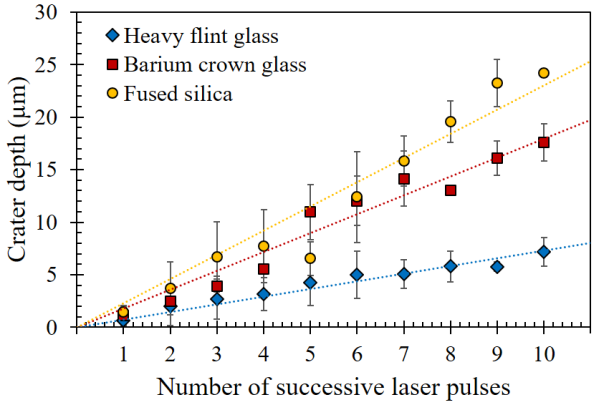

Figure 3. Crater depth vs. number of successively applied laser pulses at a fluence of 100 J/cm² on different glasses, heavy flint glass, barium crown glass and fused silica.

Since during LIBS the ablation and thus information depth is in the range of some hundreds of nanometers to some microns, SENSI-CF-LIBS can be applied for the investigation of the depth distribution of near-surface contaminations. The limiting point in terms of depth resolution is the fluence required for ensuring the ignition of a plasma in LTE (see Chapter 5) and the accompanying ablation depth. For glasses, this fluence is about 100 J/cm², where the ablation or crater depth per pulse depends on the sample material. As shown in Figure 3, quite different values may be obtained for glasses due to differences in absorption coefficients, thermal conductivity and heat capacity [ger14].

Based on the determination of the crater depth per pulse, depth-resolved SENSI-CF-LIBS allows for the investigation of near-surface phenomena on glass interfaces. Comparable and extensive studies have been performed on fused silica by several authors where other analytical methods – mainly ICP-AES and SIMS – were applied as summarized in [pfi17]. Other glasses, and especially optical glasses, are notably less considered in literature. However, due to the high variety in chemical composition, insights in manufacturing process-glass surface interactions gained for the single-component quartz glass or fused silica cannot simply be applied to other glasses of much more complex composition. Calibration-free LIBS thus turns out to be a powerful approach for filling this lag in knowledge. As an example, the fractions of several trace elements, measured for classically manufactured polished heavy flint glass via SENSI-CF-LIBS, are presented in Figure 4 as functions of depth. This glass is of specific interest since it is used for quite different applications. Due to its dispersion characteristics and its high refraction power is serves as material for corrected optical systems such as achromatic lenses [ger17] or thin ophthalmic lenses. Featuring considerable nonlinear behavior and peak Raman gain it is also of high interest for the production of photonic crystal fibers for the generation of supercontinua [hus03,kal07].

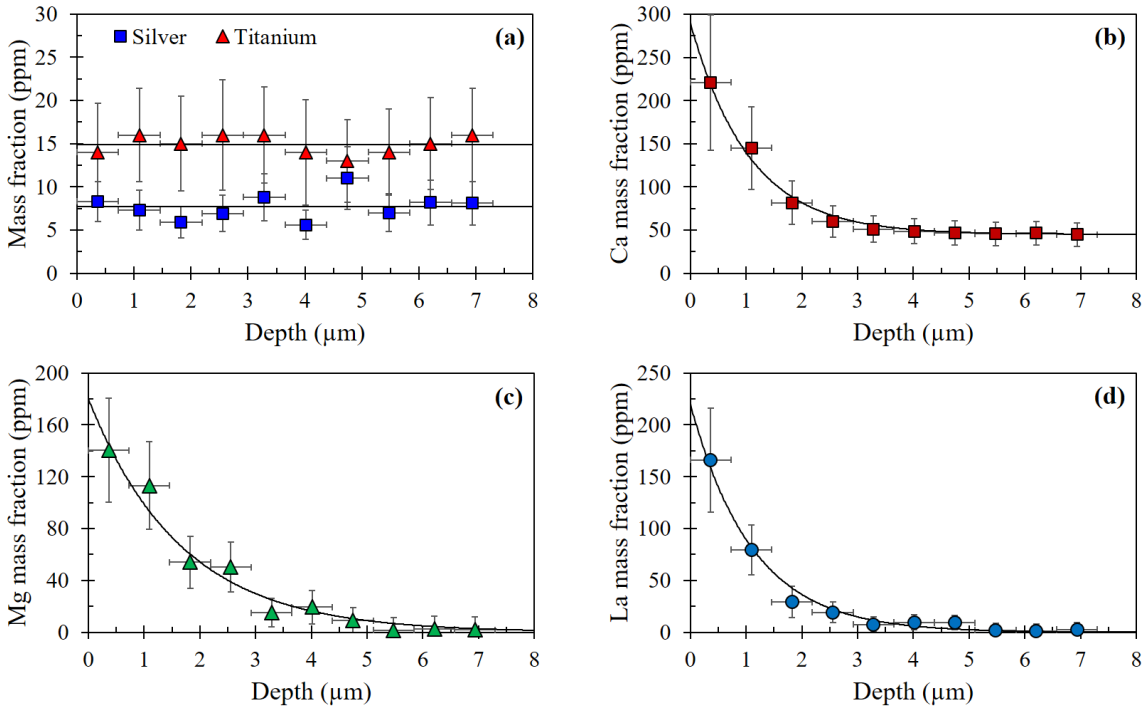

Figure 4. Mass fractions of trace elements measured as functions of depth using sensitivity-improved calibration-free LIBS in classically manufactured heavy flint glass surfaces: (a) silver and titanium, (b) calcium, (c) magnesium, and (d) lanthanum. (Adapted from [ger21]).

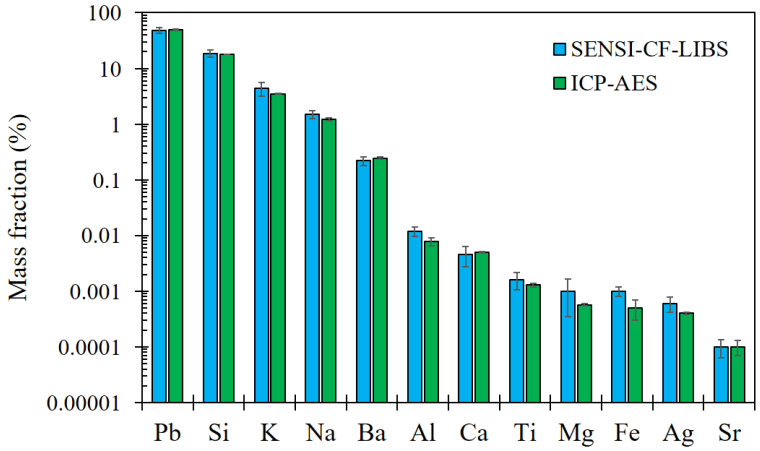

Figure 5. Comparison of mass fractions of major and minor elements within heavy flint glasses measured by sensitivity-improved calibration-free LIBS (SENSI-CF-LIBS) and inductively coupled plasma atomic emission spectroscopy (ICP-AES).

The analysis presented in Figure 5 reveals quite different effects [ger21]: First, the concentrations of silver and titanium are very low and remain constant over the measured depth range [Figure 5(a)]. These elements are well-known trace contaminants in heavy flint glasses [sto71]. Second, the calcium concentration is quite high at the glass surface but decreases exponentially with increasing depth [Figure 5(b)]. After some microns, it approaches a final, constant value of about 50 ppm, which corresponds to the content of calcium within the investigated heavy flint glass [ger14]. Third, comparable to calcium, the magnesium and lanthanum signal is high at the surface and decreases continuously. At a depth of some microns, i.e. within the glass bulk material, merely smallest traces of magnesium and no lanthanum are detected since these elements are usually not existent in heavy flint glasses. The observed elevated content of calcium, magnesium and lanthanum at the surface and its exponential decrease over depth can be explained by contamination due to diffusion in the course of the manufacturing process. Here, the elements are provided by the used water and polishing agent, cerium oxide [kat00]. The different diffusion or penetration depths of 1.1 ± 0.2 µm, 1.0 ± 0.2 µm, and 1.8 ± 0.4 µm for lanthanum, calcium, and magnesium, respectively, can be explained by the unequal atom radii and thus mobility of these elements.
This example demonstrates that SENSI-CF-LIBS has a high potential for the investigation of near-surface effects that occur at glass and optics surfaces as for example contamination by trace elements [ger21b]. Apart from manufacturing-induced contamination, long-term degradations and modifications of glass surfaces could be analyzed by this technique. One effect is the accumulation of traces from the ambient air within micro cracks in the course of time. In many cases, such aging of glass surfaces leads to the formation of a grayish and hazy surface layer. This effect is well known, but not sufficiently investigated yet. Here, and for a number of other near-surface phenomena, SENSI-CF-LIBS will most probably serve as valuable analytical measurement method for further knowledge gain in glass chemistry and optics manufacturing technology.

3.2 Accuracy of sensitivity-improved calibration-free LIBS on glasses

For any measuring method or technique used for the quantification of minor elements, traces or impurities, precision is of essential importance. The accuracy of sensitivity-enhanced calibration-free LIBS is verified by comparing the elemental fractions deduced for the glass bulk material to values measured via ICP-AES as listed in Table 1 and visualized in Figure 5.

Table 1. Mass fractions of major, minor and trace elements in heavy flint glass deduced from the calibration-free LIBS measurement for the surface and the bulk. Comparison to values measured via inductively coupled plasma atomic emission spectroscopy (ICP-AES). (Adapted from [ger21])

Element	LIBS (surface)	LIBS (bulk)	ICP-AES
Major (given in %)			
Pb	48.6	48.6	49.45
Si	18.7	18.7	18.04
K	4.4	4.4	3.50
Na	1.5	1.5	1.21
Ba	0.22	0.22	0.25
Minor/traces (given in ppm)			
Al	200	100	68
Ca	290	45	50
Ti	16	16	13
Fe	10	10	5
Ag	6	6	4
Mg	180	2	5.7
Sr	3	1	1
La	220	-	< 2
Li	40	-	< 5
Cu	6	-	< 3

It turns out that the elemental fractions deduced from the calibration-free LIBS measurements for the bulk material are in quite good accordance with the reference values measured via ICP-AES. The additional information gained by LIBS through depth-resolved measurements is precious for glass surface analysis as illustrated by the compositional differences between the bulk material and the near surface volume. This ability of LIBS analysis makes it particularity interesting as an analytical tool for quality control in the glass manufacturing industry.

4. Elemental analysis of thin films

4.1 Need of quality control in thin film manufacturing technology

Covering material surfaces with thin films is nowadays a standard in technological applications to functionalize surfaces with desired optical, electrical, mechanical or chemical properties. Among the most widespread applications are thin-film based photovoltaic devices, wear protective or tribological coatings for tools and mechanical devices, and coatings for optical surfaces or components. With the exponential increase of thin film applications over the last decades, specific techniques for their production and characterization have been developed. Beside the determination of crystallographical structure and optoelectronical properties, the measurement of the elemental composition is of great interest. Indeed, the thin film properties typically do not only depend on the major elements, but also on the minor and trace elements.

Compared to analysis of bulk matter, elemental analysis of thin films is challenging. The need of localized analysis of tiny volumes is incompatible with the standard analytical techniques such as inductively coupled plasma mass or atomic emission spectrometry (ICP-MS or ICP-AES), as these techniques require extensive sample preparation via digestion with acids [ole91,gro10]. The

techniques commonly used for the elemental analysis of thin films are Rutherford backscattering spectrometry (RBS) and X-ray photoelectron spectrometry (XPS) [sie03,jey12]. Energy-dispersive X-ray spectrometry (EDS) is suitable for the analysis of layers having micrometer thickness. Beside the need to be operated under vacuum conditions, these techniques suffer low sensitivity and elements with mass fractions below 1% are generally not accurately quantified [cli94].

Compared to the traditional techniques of thin films elemental analyses, laser-induced breakdown spectroscopy has the advantages to be operational in atmospheric conditions and to be sensitive for minor and trace element analysis. Moreover, LIBS enables localized measurements, and is therefore compatible with the industrial requirements of an analytical tool for quality control in thin film manufacturing processes.

The first thin film analysis via LIBS was reported by Cabalín and Laserna [cab01] for copper-based *Manganin* alloy coatings of 50 nm thickness, deposited by pulsed laser deposition (PLD) on silicon substrates. The authors demonstrated not only the capability of LIBS to analyze multi-elemental thin films but also the possibility of elemental mapping by scanning the laser beam over the sample surface. The quantification of the compositional measurement was based on the comparison of the measured line intensities with those obtained for the bulk *Manganin* sample, assuming equal properties of the laser-produced plasma for both the thin film and the bulk target. According to the reduced laser fluence, that was applied to minimize the probe volume depth, the signal fluctuation was large.

Semi-quantitative elemental measurements based on simple emission intensity ratio measurements were performed for other types of thin films [can05, Lee12, In13, Cho18]. Most of the analyzed layers had micrometer thickness.

To improve the measurement accuracy, Aragón et al. [ara02] proposed to include in such measurements a step for checking the relevance of self-absorption, based on calculations of plasma emission in local thermodynamic equilibrium conditions. Such considerations where then further applied to correct the measured line intensities [wid10,dav17]. Other authors applied calibration-free LIBS to compositional measurements of thin films [acq06,yua10], neglecting however self-absorption in their calculations. Calibration-free LIBS analyses that account for self-absorption were proposed later for more accurate elemental analyses of thin films [pop11,axe14].

4.2 Monitoring of thin film synthesis

Apart from the use of laser-induced breakdown spectroscopy for analysis of thin films after their fabrication, LIBS was also used for in situ monitoring during the deposition process. The purpose of such spectroscopic measurements is to investigate the physico-chemical processes within the plasma and to correlate them to the thin film properties. A better understanding of the plasma chemistry is useful for process optimization. In addition, the plasma properties derived from the spectroscopic observations, such as plasma temperature or electron density, can be used for inline process control during thin film deposition. Plasma characterization via spectroscopic observations is commonly used to monitor thin film deposition via other plasma-based methods [koi05,kou06].

In pulsed laser deposition (PLD), a pulsed laser beam is focused onto a target sample to generate an energetic vapor plume under vacuum or in a low-pressure gas atmosphere. The vaporized material propagates towards a substrate placed in front of the target. Time- and space-resolved optical emission spectroscopy was proposed to characterize the ablated vapor plume during its propagation from the target towards the substrate, measuring the propagation velocities of atomic, ionic and molecular plume species and the associated temperatures of electronic and rovibrational motions [geo92,her95,viv98]. The knowledge of the kinetic and internal energies of species arriving on the substrate were than used as input data for molecular dynamics modeling of film growth [kub97].

The so-called reactive pulsed laser deposition was proposed to deposit composite thin films of high purity. Therefore, a pure single element target is irradiated in a low-pressure reactive gas to deposit a film composed by the product of the reaction between the ablated vapor and the gas [cra93]. Monitoring of the vapor-gas chemical reactions is illustrated in Figure 6 for reactive PLD of titanium oxide.

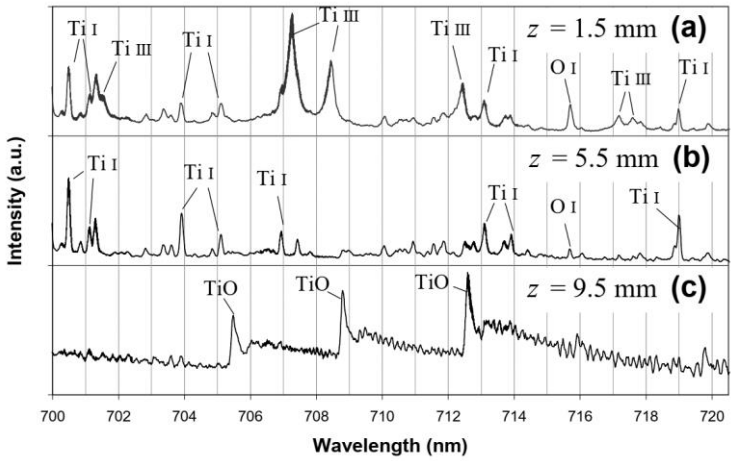

Figure 6. Plasma emission spectra recorded during pulsed laser ablation of pure titanium in low-pressure oxygen for different distances from the laser-irradiated target. The recording delay was to the maximum of plasma emission intensity for each distance. (Adapted from [her99])

According to the high plasma temperature during the early stage of plume expansion, emission of ionic transitions dominates the spectrum recorded close to the irradiated titanium target (a). With increasing distance and time of observation, the plasma temperature decreases and neutral atoms dominate the spectrum observed at a distance of 5.5 mm (b). For a further increase of the observation distance to 9.5 mm (c), molecular emission bands from the TiO Ƴ-system dominate the plasma emission spectrum, illustrating that chemical reactions in the gas phase play a significant role in the titanium oxide thin film synthesis. According to the oxygen gas pressure of 70 Pa, the distance of 9.5 mm corresponds to the stopping distance of the plume predicted by the so-called *drag force* model [geo92,her95]. The observed strong oxidation is thus due to combined effects of plasma cooling and the high rates of vapor-gas collisions. Pulsed laser deposition is usually operated at lower pressure to make sure that the ablated species or those formed by chemical reactions reach the substrate with a kinetic energy appropriate for the thin film growth process [cra93].

In addition to the kinetic energy, the internal energy of plasma species has an influence on the thin film growth process. Beside the characterization of the electronic excitation via the excitation temperatures of atoms and ions, the rovibrational excitation of molecular species impacts the mechanisms of thin film deposition. Assuming Boltzmann equilibrium distributions of the population number densities of vibrational and rotational excitation levels, the rovibrational excitation of molecular species can be characterized by the corresponding temperatures, i.e. the vibrational temperature T_{vib} and the rotational temperature T_{rot}. The temperatures T_{vib} and T_{rot} can be deduced from Boltzmann diagrams similar to the determination of the electronic excitation temperature of atoms and ions [har97]. However, the intensity measurement of the individual rotational transitions is often hindered by their interference. Therefore, more accurate measurements of the rovibrational temperatures require the simulation of the molecular emission spectrum as illustrated for the CN violet system in Figure 7.

The CN molecular emission was observed during investigations of carbon nitrite thin film synthesis via reactive PLD. The high rovibrational temperature in the vapor-gas contact front of the expanding plume is attributed to the formation of CN by recombination between carbon vapor atoms and nitrogen from the low-pressure ammonia atmosphere. According to the kinetic energy of the carbon atoms in the expanding vapor front, their recombination with nitrogen leads to CN radicals in highly excited rovibrational levels. The equality between rotational and vibrational temperatures shows that the collisional rates are large enough to ensure a collisional equilibrium between both the vibrational and the rotational degrees of freedom.

The equality $T_{vib} = T_{rot}$ was shown to apply generally in laser-produced plasmas in conditions of reactive PLD [viv98,her01]. Such plasmas are therefore expected to be in a state close to local thermodynamic

equilibrium, and modeling of plasma chemistry via the simple statistical laws of LTE was thus proposed [her02].

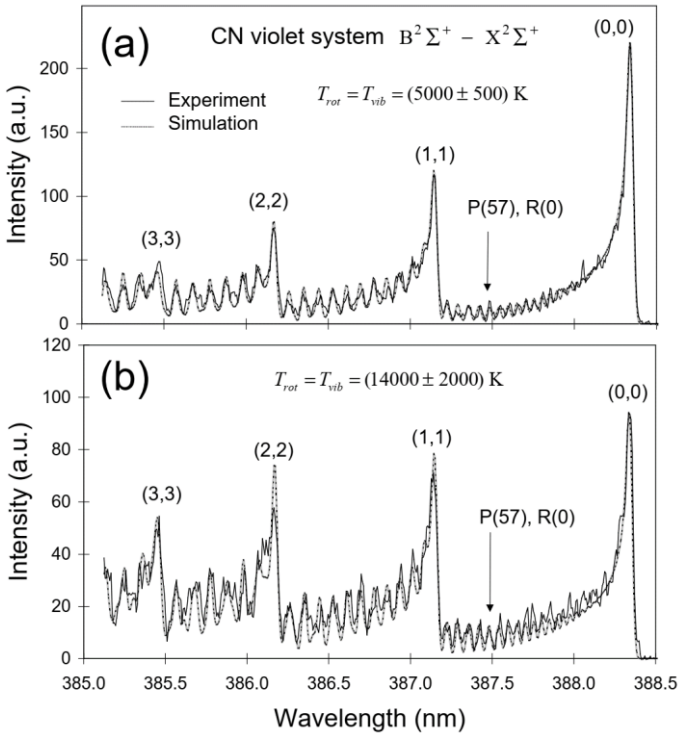

Figure 7. Measured spectra and computer simulations of the $\Delta v = 0$ vibrational sequence of the CN violet system for laser ablation of graphite in a low-pressure ammonia atmosphere. The recordings were performed at distances of 2 mm (a) and 6 mm (b) for delays of 500 ns and 300 ns, respectively. (Adapted from [viv99])

4.3 Probe volume in LIBS analysis of thin films

The irradiation conditions in laser-induced breakdown spectroscopic experiments are mainly characterized by the laser pulse energy, the pulse duration and the focusing diameter on the sample surface. The focusing geometry may also influence the processes of laser ablation and plasma generation, as the effect of plasma screening depends on the numerical aperture of laser beam focusing. The influence of the focusing geometry is thus wavelength-dependent. It may be significant for infrared laser radiation while it is mostly negligible for ultraviolet radiation. In typical LIBS experiments, laser pulses of nanosecond duration and a few mJ pulse energy are focused to a spot diameter of about 100 µm on the sample surface. The incident laser fluence of about 100 Jcm^{-2} is two orders of magnitude larger than the threshold of laser ablation for most materials. Accordingly, the ablation depth produced by a single laser pulse is of the order of 1 µm for solid materials such as glasses [ger14] and alloys [sem99].

The ablation depth can be decreased by reducing the laser fluence via downscaling the pulse energy or through defocusing. The reduction of the laser fluence lowers however the quality of the analytical signal in LIBS measurements via two effects: (i) according to the lower laser intensity, the plasma temperature and thus the analytical signal intensity are reduced. (ii) the reproducibility of plasma generation diminishes with the laser fluence [cab01].

To avoid the loss of analytical signal quality, LIBS analyses are operated with a characteristic ablation depth larger than thin films of nanometer thickness. The probe volume of LIBS analysis, that is the volume to be transformed into a hot plasma, is typically smaller than the ablated volume as illustrated schematically in Figure 8. Accordingly, the probe depth is smaller than the ablated depth. The ratio between both depths is generally unknown. It depends on the sample material and the laser irradiation conditions. For films having a thickness of the order of 100 nm or thinner, the probe volume is

supposed to include atoms from the substrate as illustrated in Figure 8(b). In that situation, calibrated LIBS is difficult to apply as the contribution of the substrate may alter the plasma properties. Compositional measurements of thin films are therefore a challenging application of calibration-free analysis.

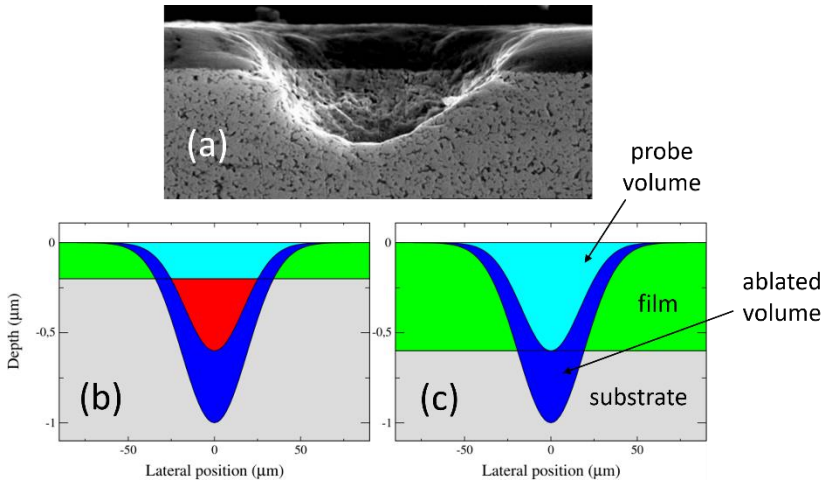

Figure 8. (a) Scanning electron microscopic image of a cross section cut through a laser-produced crater in cobalt -cemented tungsten carbide covered with a TiCN coating (Adapted from [dum04]). (b, c) Cross section scheme of laser produced craters in samples covered with thin films of different thicknesses illustrating the impact of film thickness on the composition of the probe volume.

4.4 Accurate analysis of thin films via calibration-free LIBS

4.4.1 Analyses in ambient air

Most approaches of calibration-free LIBS analysis are based on the assumption of a spatially uniform plasma, characterized by unique values of temperature and electron density. Although this assumption was shown to apply in appropriate experimental conditions and in particular for LIBS experiments in argon background gas [her17], it is generally not valid for LIBS measurements in ambient air [her14]. Compared to an inert gas such as argon, a molecular gas like air interacts with the laser-ablated vapor plume through inelastic collisions during which the numerous vibrational and rotational levels are excited. This leads to cooling of the vapor in the vicinity of the vapor-gas contact front and thus to temperature gradients in the vapor plume. The simplest approach to account for these gradients is to describe the plasma by dividing it in two zones, representing the hot plasma core and the border of lower temperature (see Figure 9).

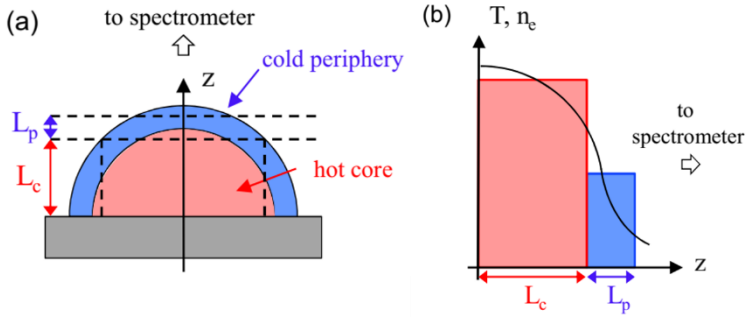

Figure 9. (a) Scheme of the hemispherical ablation plume composed of hot core and cold periphery. (b) Approximate description of spatial distributions of plasma properties by two zones of different thermodynamic state. (Adapted from [her15])

In that case, the spectral radiance of the plasma in LTE can be computed via the following analytical solution of the radiation transfer equation [her98]

$$B_\lambda = U_p(1 - e^{-\tau_p}) + U_c(1 - e^{-\tau_c})e^{-\tau_p}, \quad (1)$$

where U is the blackbody spectral radiance and τ is the optical thickness. The subscripts c and p stand for the core and the peripheral plasma volumes, respectively. Details on the calculation of the spectral radiance and the implementation in the calibration-free LIBS measurement algorithm can be found in [axe14,her15] and in chapter 5 of this book.

Thin film analyses via calibration-free LIBS in air are demonstrated for indium zinc oxide (IZO). The plasma emission spectrum is characterized by a few spectral lines only as shown in Figure 10(a). All transitions of indium have high intensity and suffer strong self-absorption. In that case, a means to reduce the amount of self-absorption is given by setting the delay between the laser pulse and the detector gate to a short time. The strong plasma ionization leads then to the reduction of self-absorption of transition from neutral atoms via two distinguished mechanisms: (i) according to the large stage of ionization, the number density of atoms is reduced; (ii) the optical thickness is further reduced due to Stark broadening of the spectral line profile resulting from the large electron density.

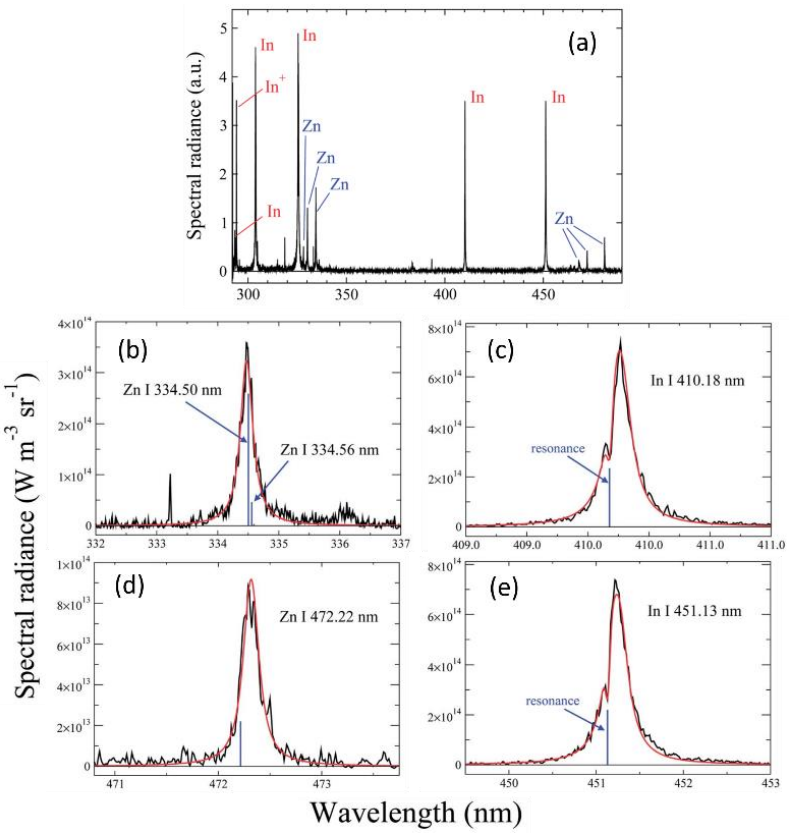

Figure 10. (a) LIBS spectrum recorded during IZO thin film ablation in air for a delay of 400 ns between the laser pulse and the observation gate. (b-e) Comparison to the spectral radiance of Zn and In transitions computed according to Equation (1). (Reproduced from Ref. [axe14] with permission from the Royal Society of Chemistry)

A delay of 400 ns was chosen for the analysis of the indium zinc oxide thin film. The choice was guided by a compromise given by lowest optical thickness of the selected analytical lines for indium [see Figure 10(c) and (e)] and the highest signal-to-noise ratio of the lower intensity zinc transitions [see Figure 10(b) and (d)]. The comparison of the measured spectrum to the spectra radiance computed for a nonuniform plasma according Equation (1) indicates that the plasma border mainly contributes to the plasma emission spectrum through absorption. Indeed, the absorption dips of the indium transitions are located at their resonance wavelengths, showing thus that the electron density in the cold border

is small compared to the value in the plasma core volume. The zinc transitions are characterized by symmetric, but Stark-shifted line profiles. This shows that the contribution of emission from the plasma border is negligible, and these lines of negligible self-absorption could be described by a simple model of a uniform plasma [her14].
The two resonance lines of indium displayed in Figure 10(c) and (e) have significant different optical thickness, and the simulation of both lines are useful for the evaluation of the accuracy of the applied two zone model. The quality of simulation is fair for both transitions, a small deviation between measured and computed spectrum is however observed for the absorption dip of the In I 410.18 nm line. The decay may be attributed to uncertainties of the Stark broadening parameters that have been assumed to be temperature-invariant for simplification [axe14].
The atomic fraction of indium measured via calibration-free LIBS for a thin film produced by so-called combinatorial pulsed laser deposition is displayed in Figure 11 as a function of the longitudinal position on the sample. Combinatorial PLD is a variant of pulsed laser deposition where two targets of different composition are irradiated simultaneously to deposit a thin film with a compositional gradient [chr01]. The fraction of indium measured via calibration-free LIBS is shown to be in good agreement with the reference values measured via energy dispersive X-ray spectroscopy.

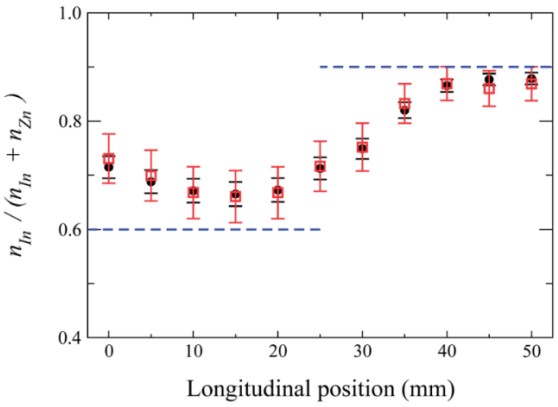

Figure 11. Atomic fraction of indium compared to the total metal content within the indium zinc oxide thin film versus the longitudinal position on the sample. The fractions measured by LIBS and EDS are represented by empty red and filled black symbols, respectively. The dashed lines represent the indium fractions of the targets used for thin film synthesis by combinatorial PLD. (Reproduced from Ref. [axe14] with permission from the Royal Society of Chemistry)

4.4.2 Analyses in argon background gas

The analytical performance of calibration-free LIBS measurements is improved when the samples are irradiated in argon background gas. Beside the gain in signal-to-noise ratio, the spatially uniform character of the laser-produced plasma is of great interest as it enables accurate and robust modeling of the plasma emission spectrum [her17]. The irradiation in argon background gas was therefore chosen to evaluate the capability of analyzing multi-elemental thin films of thickness well below the depth of laser ablation.
The first step in the computation scheme of the calibration-free LIBS analysis consists in the calculation of the LTE plasma composition as a function of temperature, electron density and the elemental fractions [her10, ger14] (see Chapter 5). Such calculations can be performed by solving numerically the system of Saha equations with the neutrality equation as closure relation [her02]. The computation is quasi instantaneous, even when a multi-elemental plasma composed of neutral and charged atomic and molecular species is considered.
The composition of a plasma in LTE with the elemental composition of a nickel–chromium–molybdenum alloy is displayed in Figure 12 as a function of temperature. Here, the dependence of electron density versus temperature, deduced from measurements for different delays between the

laser pulse and the detector gate, was applied as boundary condition [her19]. Thus, the composition computed for each temperature corresponds to the state of the plasma at a given time. The highest temperature values correspond to the earliest delays, where the plasma density is large, and accordingly the pressure is high. During the plume expansion, temperature, density and pressure decrease. The plume reaches a maximum volume at a delay of several microseconds. This corresponds to a minimum pressure, similar to the expansion dynamics of a classical explosion [her18].

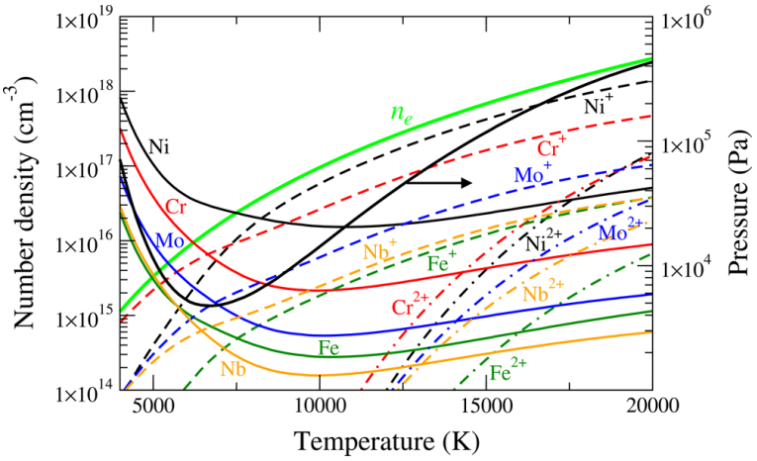

Figure 12. Number densities of species as functions of temperature computed for a plasma in LTE with the elemental composition of a nickel–chromium–molybdenum alloy (Inconel 625). The calculations were performed for the $n_e = f(T)$ dependence deduced from the measurements. The calculated kinetic pressure is presented with respect to the secondary *y*-axis. (Adapted from [her19])

The alloy-composing elements are characterized by rich emission spectra. Thus, to minimize measurement errors due to line-interference, the calibration-free analyses should be operated with spectra recorded with a large delay, for which the spectral lines are narrow according to reduced Stark broadening. The electron density should however be large enough so that the validity condition of local thermodynamic equilibrium is satisfied. The validity condition is rather relaxed for most metals and the LTE state is established for measurement delays up to several microseconds [her15]. Based on a detailed evaluation of the calibration-free LIBS measurement errors, the most appropriate measurement delay was found to be situated in the time interval from 1 to 2 µs [her19]. At this time, the temperature is close to 10,000 K and the dominating plasma species are singly-charged ions and neutral atoms (see Figure 12).

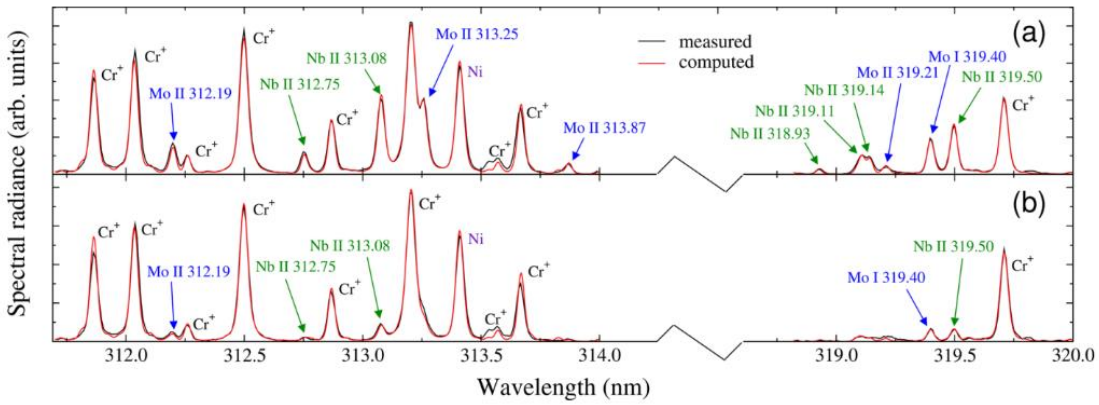

Figure 13. Measured and computed spectral radiance of transitions from chromium, molybdenum, niobium, and nickel. The recordings were performed during ablation of (a) the bulk alloy sample and (b) the deposited thin film for $t = 1.25 \pm 0.25$ µs. (Adapted from [her19])

Spectra recorded in argon for the bulk Inconel target and the thin film deposited via PLD are displayed in Figure 13 together with the spectra computed for a uniform LTE plasma. The displayed spectral windows show transitions of the major elements. Compared to line intensities observed for the bulk target, the spectral lines of molybdenum and niobium have significantly lower intensities in the spectrum recorded for the thin film.

The mass fractions deduced from the calibration-free LIBS analysis are displayed in Figure 14 for both the Inconel bulk target and the thin film. Similar values are observed for all elements except molybdenum, niobium and calcium. The reduced abundance of calcium within the thin film was attributed to a nonuniform distribution of calcium in the target. Indeed, in-depth measurements via calibration-free LIBS evidenced that the mass fraction of calcium is much larger at the surface of the Inconel target than in the bulk (see [her19], Supporting Information). During thin film deposition via PLD, the target is continuously rotated while it is irradiated with thousands of laser pulses. Accordingly, the total ablation depth is much larger than the depth that characterizes the calcium enrichment in the near surface volume. As the LIBS analysis of the Inconel target were performed on the virgin, non-irradiated surface, these measurements were representative of the near-surface volume of large calcium content. Contrarily, the thin film was only partly deposited with calcium-enriched material from the near-surface volume and most of the deposited material originated from the calcium-poor bulk alloy.

The change of the mass fractions of molybdenum and niobium, that were found to be about four times lower in the thin film, was confirmed by RBS analysis as shown in Figure 14(b).

Non-stoichiometric mass transfer in pulsed laser deposition was often reported [arn99,kla16]. The possible causes are: (i) non-stoichiometric target vaporization; (ii) segregation in the vapor plume; and (iii) element-dependent sticking probability on the substrate surface. In the here reported case, non-stoichiometric target vaporization may be excluded as it would lead to the enrichment of the target with molybdenum and niobium, and therefore counterbalance non-stoichiometric target vaporization in case of multiple laser irradiation of the same site on the surface.

However, multi-pulse laser irradiation generated a columnar structure (see [her19], Supporting Information) that is known to cause a deflection of the plume symmetry axis from the surface normal towards the laser optical axis, typically at 45° from the surface normal [cul06]. In case of strong plume deflection, the heaviest atoms, characterized by the narrowest angular distribution around the plume symmetry axis, will be mostly deposited beside the substrate and the deposited thin film is thus heavy-atom deficient.

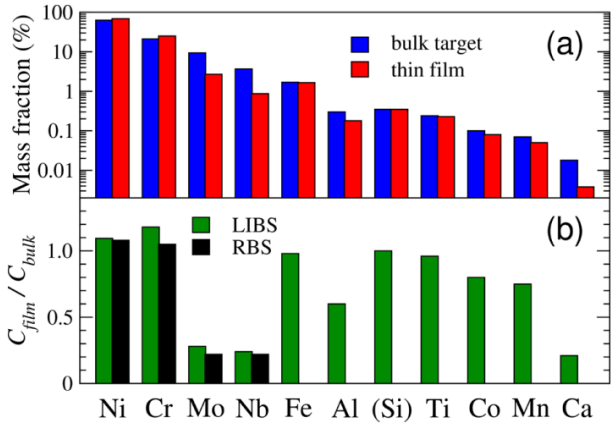

Figure 14. (a) Elemental compositions of the bulk alloy target and the thin film deduced from the spectra recorded for t = 1.25 and 2.50 µs. (b) The deduced fraction ratio C_{film} / C_{bulk} is compared to the ratio measured via RBS for the most-abundant elements. (Adapted from [her19])

5. Conclusion

The results presented in this book chapter demonstrate that calibration-free laser-induced breakdown spectroscopy represents a powerful solution for the challenging problem of elemental analyses of optical surfaces and thin films, combining the capability of quantifying major, minor and trace elements with the ability of performing rapid measurements of tiny volumes. For analysis in ambient air, the simplest calibration-free approach, based on the assumption of uniform equilibrium plasma, is applicable as long as analytical spectral lines of negligible self-absorption are considered. In the opposite case, absorption at the cold plasma border has to be considered, and a two-zones model is shown to enable accurate compositional measurements. The analytical performance is increased for analysis in argon background gas, in particular due to the spatially uniform plasma distribution that enables accurate and robust modeling. In-depth measurements via the application of successive laser pulses on the same irradiation site are shown to be an efficient tool to investigate trace element impurities in the near surface volume. This is of specific interest for the clarification of phenomena on glass surfaces and especially manufacturing-induced contaminants and defects.
Calibration-free LIBS measurements are foreseen to enable accurate analysis of thin films having thicknesses down to values of the order of 10 nm, given that the film-composing elements do not occur in the substrate. Challenges of such measurements are the reduction of the probe volume depth without loss of the validity condition of the calibration-free LIBS model. Other issues concern the need of accurate spectroscopic data that are still missing for many elements, and improvements of the CF-LIBS procedures such as a rapid measurement of the apparatus response function through the use of the laser-induced plasma as a radiation standard [tal21].

Acknowledgements

The research leading to the results presented in this chapter has received funding from the EC's Seventh Framework Programme under grant agreement No 284464 Laserlab-Europe (Project CNRS-LP3001916) and the European Union's Horizon 2020 research and innovation programme under grant agreement No 654148 Laserlab-Europe (Project CNRS-LP3002491).

References

[acq06] Acquaviva, S., D'Anna, E., De Giorgi, M. L., and Moro, F. (2006). Laser-induced breakdown spectroscopy for compositional analysis of multi-elemental thin films. *Spectrochimica Acta Part B* 61:810–816.
[ara02] Aragón, C., Madurga, V., and Aguilera, J. A. (2002). Application of laser-induced breakdown spectroscopy to the analysis of the composition of thin films produced by pulsed laser deposition. *Applied Surface Science* 197-198:217-223.
[arn99] Arnold, C. B. and Aziz, M. J. (1999). Stoichiometry issues in pulsed-laser deposition of alloys grown from multicomponent targets. *Applied Physics A* 69:S23–S27.
[axe14] Axente, E., Hermann, J., Socol, G., Mercadier, L., Beldjilali, S.A., Cirisan, M., Luculescu, C.R., Ristoscu, C., Mihailescu, I.N., and Craciun, V. (2014). Accurate analysis of indium–zinc oxide thin films via laser-induced breakdown spectroscopy based on plasma modeling. *Journal of Analytical Atomic Spectrometry* 29:553–564.
[ban17] Banerjee, J., Bojan, V., Pantano, C.G., and Kim, S.H. (2018). Effect of heat treatment on the surface chemical structure of glass: Oxygen speciation from in situ XPS analysis. *Journal of the American Ceramic Society* 101:644–656.
[bau13] Baudelet, M. and Smith, B.W. (2013). The first years of laser-induced breakdown spectroscopy. *Journal of Analytical Atomic Spectrometry* 28;624–629.
[ben75] Benninghoven, A. (1975). Development in secondary ion mass spectroscopy and applications to surface studies. *Surface Science* 53(1):596–625.
[bul02] Bulajic, D., Corsi, M., Cristoforetti, G., Legnaioli, S., Palleschi, V., Salvetti, A., and Tognoni, E. (2002). A procedure for correcting self-absorption in calibration free-laser induced breakdown spectroscopy. *Spectrochimica Acta Part* B 57:339–353.

[cab01] Cabalín, L. M. and Laserna, J. J. (2001). Surface stoichiometry of manganin coatings prepared by pulsed laser deposition as described by laser-induced breakdown spectrometry. *Analytical Chemistry* 73:1120-1125.
[cah08] Chakraborty, P. (2008). Ultra-high depth resolution SIMS for the interface analysis of complex low-dimensional structures. *Nuclear Instruments and Methods in Physics Research Section B* 266(8):1858–1865.
[can05] Caneve, L., Colao, F., Sarto, F., Spizzichino, V., and Vadrucci, M. (2005). Laser-induced breakdown spectroscopy as a diagnostic tool for thin films elemental composition. *Spectrochimica Acta Part B* 60(7–8):1098–1102.
[che18] Chen, C.-T., Banaru, D., Sarnet, T., and Hermann, J. (2018). Two-step procedure for trace element analysis in food via calibration-free laser-induced breakdown spectroscopy. *Spectrochimica Acta Part B* 150:77–85.
[cho18] Choi, J.-H., Lee, H.-J., Lee, S.-H., et al. (2018). Effects of spot size variation on the laser induced breakdown spectroscopy analysis of Cu(In,Ga)Se2 solar cell. *Thin Solid Films* 660:314–319.
[chr01] Christen, M. H., Silliman, S. D., and Harshavardhan, K. S. (2001). Continuous compositional-spread technique based on pulsed-laser deposition and applied to the growth of epitaxial films. *Review of Scientific Instruments* 72:2673–2678.
[ciu99] Ciucci, A., Corsi, M., Palleschi, V., Rastelli, S., Salvetti, A., and Tognoni, E. (1999). New procedure for quantitative elemental analysis by laser-induced plasma spectroscopy. *Applied Spectroscopy* 53:960–964.
[cli94] Climent-Font, A., Fernández-Jiménez, M. T., Wätjen, U., and Perrière, J. (1994*).* RBS - an analytical technique for elemental characterization of standards – advantages and limits of application. *Nuclear Instruments and Methods in Physics Research Section A* 353:575−578.
[cra93] Craciun, V., Craciun, D., and Boyd, I. W. (1993). Reactive pulsed laser deposition of thin films. *Materials Science and Engineering B* 18:178-180.
[cul06] Cultrera, L., Zeifman, M. I., and Perrone, A. (2006). Investigation of liquid droplets, plume deflection, and a columnar structure in laser ablation of silicon. *Physical Review B* 73:075304 1-5.
[dal10] D'Alfonso, A.J., Freitag, B., Klenov, D., and Allen, L.J. (2010). Atomic-resolution chemical mapping using energy-dispersive x-ray spectroscopy. *Physical Review B* 81:100101(R).
[dav17] Davari, S.A., Hu, S., Pamu, R., and Mukherjee, D. (2017). Calibration-free quantitative analysis of thin-film oxide layers in semiconductors using laser induced breakdown spectroscopy (LIBS). *Journal of Analytical Atomic Spectrometry* 32:1378–1387.
[duc02] Duckworth, D.C, Morton, S.J., Bayne, C.K., Koons, R.D., Montero, S., and Almirall, J.R. (2002). Forensic glass analysis by ICP-MS: a multi-element assessment of discriminating power via analysis of variance and pairwise comparisons. *Journal of Analytical Atomic Spectrometry* 17:662–668.
[dum04] Dumitru, G., Romano, V., Weber, H.P. et al. (2004) Femtosecond laser ablation of cemented carbides: properties and tribological applications*. Applied Physics A* 79:629-632.
[ekt00] Ektessabi, A.M. and Hakamata, S. (2000). XPS study of ion beam modified polyimide films. *Thin Solid Films* 377–378: 621–625.
[fal06] Falcone, R., Sommariva, G., and Verita, M. (2006). WDXRF, EPMA and SEM/EDX Quantitative Chemical Analyses of Small Glass Samples. *Microchimica Acta* 155:137–140.
[fu19] Fu, H., Ni, Z., Wang, H., Jia, J., and Dong, F. (2019). Accuracy improvement of calibration-free laser-induced breakdown spectroscopy. *Plasma Science and Technology* 21:034001.
[geo92] Geohegan, D. B. (1992). Physics and diagnostics of laser ablation plume propagation for high-T, superconductor film growth. *Thin Solid Films* 220:138-145.
[ger12] Gerhard, C., Tasche, D., Brückner, S., Wieneke, S., and Viöl, W. (2012). Near-surface modification of optical properties of fused silica by low-temperature hydrogenous atmospheric pressure plasma. *Optics Letters* 37(4):566–568.
[ger14] Gerhard, C., Hermann, J., Mercadier, L., Loewenthal, L., Axente, E, Luculescu, C.R., Sarnet, T., Sentis, M., and Viöl, W (2014). Quantitative analyses of glass via laser-induced breakdown spectroscopy in argon. *Spectrochimica Acta Part B* 101:32–45.
[ger17] Gerhard, C. (2017). *Optics Manufacturing: Components and Systems*. Boca Raton: CRC Taylor & Francis.
[ger17a] Gerhard, C., Tasche, D., Munser, N., and Dyck, H. (2017). Increase in nanosecond laser-induced damage threshold of sapphire windows by means of direct dielectric barrier discharge plasma treatment. *Optics Letters* 42(1): 49–52.
[ger17b] Gerhard, C., Tasche, D., Uteza, O., and Hermann, J. (2017). Investigation of nonuniform surface properties of classically-manufactured fused silica windows. *Applied Optics* 56(26): 7427–7434.
[ger21] Gerhard, C., Taleb, A., Pelascini, F. and Hermann, J. (2021). Quantification of surface contamination on optical glass via sensitivity-improved calibration-free laser-induced breakdown spectroscopy. *Applied Surface Science* 537: 147984 (7pp)

[ger21b] Gerhard, C. (2021). Towards laser-based calibration-free quantification of trace elements. *Optics* 2(1):43–44.
[gro10] Groh, S., Diwakar, P. K., Garcia, C. C. et al. (2010). 100% efficient sub-nanoliter sample introduction in laser-induced breakdown spectroscopy and inductively coupled plasma spectrometry: implications for ultralow sample volumes. *Analytical Chemistry* 82:2568−2573.
[har97] Harilal S. S., Issac R. C., Bindhu C. V. et al. (1997). Time resolved study of CN band emission from plasma generated by laser irradiation of graphite. *Spectrochimica Acta Part A* 53:1527-1536.
[hat97] Hattori, A. (1997). Measurement of glass surface contamination. *Journal of Non-Crystalline Solids* 218:196–204.
[hau93] Hauert, R., Patscheider, J., Tobler, M., and Zehringer, R. (1993). XPS investigation of the a-C:H/Al interface. *Surface Science* 292(1–2):121–129.
[her01] Hermann, J., Coursimault, F., Motret, O. et al. (2001) Investigation of silicon oxide emission spectra observed in a pulsed discharge and a laser-induced plasma. *Journal of Physics B* 34:1917-1927.
[her02] Hermann, J. and Dutouquet, C. (2002). Local thermal equilibrium plasma modeling for analyses of gas-phase reactions during reactive-laser ablation. *Journal of Applied Physics* 91:10188-10193.
[her10] Hermann, J., Mercadier, L., Mothe, E. et al. (2010). On the stoichiometry of mass transfer from solid to plasma during pulsed laser ablation of brass. *Spectrochimica Acta Part B* 65:636-641.
[her14] Hermann, J., Gerhard, C., Axente, E., and Dutouquet, C. (2014). Comparative investigation of laser ablation plumes in air and argon by analysis of spectral line shapes: Insights on calibration-free laser-induced breakdown spectroscopy. *Spectrochimica Acta Part B* 100:189–196.
[her15] Hermann, J., Lorusso, A., Perrone, A. et al. (2015) Simulation of emission spectra from nonuniform reactive laser-induced plasmas. *Physical Review E* 92:053103 1-15.
[her17] Hermann, J., Grojo, D., Axente, E., Gerhard, C., Burger, M., and Craciun, V. (2017). Ideal radiation source for plasma spectroscopy generated by laser ablation. *Physical Review E* 96(6):53210
[her18] Hermann, J., Axente, E., Craciun, V., et al. (2018) Evaluation of pressure in a plasma produced by laser ablation of steel. *Spectrochimica Acta Part B* 143:63-70.
[her19] Hermann, J., Axente, E., Pelascini, F., and Craciun, V. (2019) Analysis of multi-elemental thin films via calibration-free laser-induced breakdown spectroscopy. *Analytical Chemistry* 91:2544-2550.
[her95] Hermann, J., Thomann, A. L., Boulmer-Leborgne, C. et al. (1995). Plasma diagnostics in pulsed TiN layer deposition. *Journal of Applied Physics* 77:2928-2936.
[her99] Hermann J. and Dutouquet C. (1999). Analyses of gas-phase reactions during reactive laser ablation using emission spectroscopy. *Journal of Physics D* 32:2707-2713.
[hod19] Hodgkinson, A.K, Röhrs, S., Müller, K., and Reiche, I. (2019). The use of Cobalt in 18th Dynasty Blue Glass from Amarna: the results from an on-site analysis using portable XRF technology. *STAR: Science & Technology of Archaeological Research* 5(2)36–52.
[hol01] Holland, D., Gee, I.A., Mekki, A, and McConville, C.F. (2001). Role of surface science in the determination of glass structure. *Physics and Chemistry of Glasses* 42(3):247–254.
[hus03] Husakou, A. and Herrmann, J. (2003). Supercontinuum generation in photonic crystal fibers made from highly nonlinear glasses. *Applied Physics B* 77:227–234.
[in13] In, J.-H., Kim, C.-K., Lee, S.-H., and Jeong, S. (2013). Reproducibility of CIGS thin film analysis by laser-induced breakdown spectroscopy. *Journal of Analytical Atomic Spectrometry* 28:473–481.
[jab88] Jablonski, A., Lesiak, B., Ebel, H., and Ebel, M.F. (1988). Matrix dependence of elastic scattering effects in quantitative AES and XPS. *Surface and Interface Analysis* 12: 87–92.
[jem02] Jembrih-Simbürger, D., Neelmeijer, C., Schalm, O., Fredrickx, P., Schreiner, M., De Vis, K., Mäder, M., Schryverse, D., and Caenf, J. (2002). The colour of silver stained glass—analytical investigations carried out with XRF, SEM/EDX, TEM, and IBA. *Journal of Analytical Atomic Spectrometry* 17:321–328.
[jey12] Jeynes, C., Barradas, N. P., and Szilágyi, E. (2012). Accurate Determination of Quantity of Material in Thin Films by Rutherford Backscattering Spectrometry. *Analytical Chemistry* 84:6061−6069.
[jie90] Jie, L. and Chao, X. (1990). XPS examination of tin oxide on float glass surface. Journal of Non-Crystalline Solids 119(1): 37–40.
[kaa18] Kaasika, V.P., Lipovskii, A.A., Raskhodchikov, D.V., Reshetov, I.V., and Tagantsev D.K. (2019). How to reveal the correct elemental concentration profiles in poled multicomponent silicate glasses from the data of secondary ion mass spectrometry (SIMS). *Journal of Non-Crystalline Solids* 503–504:397–399.
[kal07] Kalashnikov, V.L., Sorokin, E., and Sorokina, I.T. (2007). Raman effects in the infrared supercontinuum generation in soft-glass PCFs. *Applied Physics B* 87:37–44.

[kan12] Kanngießer, B., Malzer, W., Mantouvalou, I., Sokaras, D. and Karydas, A.G. (2012). A deep view in cultural heritage—confocal micro X-ray spectroscopy for depth resolved elemental analysis. *Applied Physics A* 106:325–338.
[kat00] Kato, K., Yoshioka, T., and Okuwaki A. (2000). Study for recycling of ceria-based glass polishing powder. *Industrial & Engineering Chemistry Research* 39:943–947.
[kla16] Klamt, C., Dittrich, A., Jaquet, B., Eberl, C., et al. (2016). Largest possible deviations from stoichiometry transfer during pulsed laser deposition. *Applied Physics A* 122:701 1-5.
[koi05] Koizumia, T., Wada, J., Araki, T. et al. (2005). Optical emission spectroscopy during InN growth by ECR–MBE. *J. Crystal Growth* 275:e1073–e1077.
[koo91] Koons, R.D., Peters, C.A, and Rebbert, P.S. (1991). Comparison of Refractive Index, Energy Dispersive X-Ray Fluorescence and Inductively Coupled Plasma Atomic Emission Spectrometry for Forensic Characterization of Sheet Glass Fragments. *Journal of Analytical Atomic Spectrometry* 6:451–456.
[kou06] Koufaki, M., Sifakis, M., Iliopoulos, E. et al. (2006). Optical emission spectroscopy during fabrication of indium-tin-oxynitride films by RF-sputtering. *Applied Surface Science* 253:405–408.
[koz92] Kozhukharov, V., Stoyanova, G., Danova, D., and Atanasov, S. (1992). Quantitative chemical analysis of borosilicate glasses by the inductively coupled plasma-atomic emission spectroscopy method. *Journal of Materials Science Letters* 11:1702–1704.
[kub97] Kubo, M., Oumi, Y., Miura, R., et al. (1997). Atomic control of layer-by-layer epitaxial growth on SrTiO3(001): Molecular-dynamics simulations. *Physical Review B* 56:13535-13542.
[lag14] Lagrange, J. F., Hermann, J., Wolfman, J., and Motret, O. (2014). Time-resolved spatial distribution of plasma in the ablation of a $Ba_{0.6}Sr_{0.4}TiO_3$ target by 25 ns KrF ultraviolet laser. *Journal of Applied Physics* 116:133303.
[lam02] Lampman, S.R. (2002). *Fatigue and fracture*. Materials Park: ASM International.
[lee12] Lee, S. H., Shim, H. S., Kim, C. K. et al. (2012). Analysis of the absorption layer of CIGS solar cell by laser-induced breakdown spectroscopy. *Applied Optics* 51: B115-B120.
[lin63] Lineweaver, J.L. (1963). Oxygen outgassing caused by electron bombardment of glass. *Journal of Applied Physics* 34: 1786–1791.
[liu12] Liu, S., Li, Q.H., Gan, F., Zhang P., and Lankton, J.W. (2012). Silk Road glass in Xinjiang, China: chemical compositional analysis and interpretation using a high-resolution portable XRF spectrometer. *Journal of Archaeological Science* 39:2128–2142.
[mah17] Mahdi, D. and Chaabi, A. (2017). Analytical description of SIMS depth resolution with different ions dose irradiation. *AIP Conference Proceedings* 1809:020033.
[mar14] Marschall, H.R. and Monteleone, B.D. (2014). Boron Isotope Analysis of Silicate Glass with Very Low Boron Concentrations by Secondary Ion Mass Spectrometry. *Geostandards and Geoanalytical Research* 39(1):31–46.
[nak09] Nakano, K. and Tsuji, K. (2009). Nondestructive elemental depth profiling of Japanese lacquerware 'Tamamushi-nuri' by confocal 3D-XRF analysis in comparison with micro GE-XRF. *X-Ray Spectrometry* 38 (5):446–450.
[nea05] Neauport, J., Lamaignere, L., Bercegol, H., Pilon, F., and Birolleau, J.-C. (2005). Polishing-induced contamination of fused silica optics and laser induced damage density at 351 nm. *Optics Express* 13(25):10163-10171.
[nea09] Neauport, J., Ambard, C., Cormont, P., Darbois, N., Destribats, J., Luitot, C., and Rondeau, O. (2009). Subsurface damage measurement of ground fused silica parts by HF etching techniques. *Optics Express* 17: 20448–20456.
[neg15] Negre, E.v Motto-Ros, V., Pelascini, F., Lauper, S., Denis, D., and Yu, J. (2015). On the performance of laser-induced breakdown spectroscopy for quantitative analysis of minor and trace elements in glass. *Journal of Analytical Atomic Spectrometry* 30:417–425.
[ole91] Olesik, J. W. (1991). Elemental Analysis Using ICP-OES and ICP/MS. *Analytical Chemistry* 63:12A−21A.
[ony93] Onyiriuka, E.C. (1993). Zinc phosphate glass surfaces studied by XPS. *Journal of Non-Crystalline Solids* 163(3):268–273.
[owe10] Owens, T., Mao, S.S., Canfield, E.K., Grigoropoulos, C.P., Mao, X., and Russo, R.E. (2010). Ultrafast thin-film laser-induced breakdown spectroscopy of doped oxides. *Applied Optics* 49(13):C67–C69.
[per87] Perrière, J. (1987). Rutherford backscattering spectrometry. *Vacuum* 37(5–6): 429–432
[pfi17] Pfiffer, M., Longuet, J.-L., Labrugère, C., Fargin, E., Bousquet, B., Dussauze, M., Lambert, S., Cormont, P., and Neauport J. (2017). Characterization of the polishing-induced contamination of fused silica optics. *Journal of the American Ceramic Society* 100:96–107.

[pop11] Popescu, A.C., Beldjilali, S., Socol, G., et al. (2011). Analysis of indium zinc oxide thin films by laser-induced breakdown spectroscopy. *Journal of Applied Physics* 110:083116 1-8.
[ran18] Rani, R., Panda, K., Kumar, N., Sankaran, K. J., Ganesan, K., and Lin, I.-N. (2018). Tribological Properties of Ultrananocrystalline Diamond Films in Inert and Reactive Tribo-Atmospheres: XPS Depth-Resolved Chemical Analysis. *The Journal of Physical Chemistry* 122(15):8602–8613.
[reg16] Regier, M.E., Hervig, R.L., Myers, M.L., Roggensack, K., and Wilson, C.J.N. (2016). Analyzing nitrogen in natural and synthetic silicate glasses by secondary ion mass spectrometry. *Chemical Geology* 447: 27–39.
[ric96] Rickerby, D.G. (1996). Barriers to energy dispersive spectrometry with low energy X-rays. *Mikrochimica Acta Supplementa* 13: 493–500.
[sch12] Schenk, E.R and Almirall, J.R. (2012). Elemental analysis of glass by laser ablation inductively coupled plasma optical emission spectrometry (LA-ICP-OES). *Forensic Science International* 217(1-3):222–228.
[sem99] Semerok, A., Chaléard, C., Detalle, V., et al. (1999). Experimental investigations of laser ablation efficiency of pure metals with femto, pico and nanosecond pulses. *Applied Surface Science* 138-139:311-314.
[sie03] Sie, S. H. Surface Analysis Methods in Materials Science. In O'Connor, D. J., Sexton, B. A., Smart, R. S. C., editors, *Springer Series in Surface Sciences*, volume 23, pages 229−246. Springer, Berlin, 2003.
[sto71] Stockham, J.D. (1971). The composition of glass furnace emissions. *Journal of the Air Pollution Control Association* 21:713-715.
[sun15] Sun, T. and Ding, X. (2015). Confocal X-ray technology based on capillary X-ray optics. *Reviews in Analytical Chemistry* 34(1–2): 45–59.
[sur15] Suratwala, T., Steele, W., Wong, L., Feit, M.D., Miller, P.E., Dylla-Spears, R., Shen, N., and Desjardin, R. (2015). Chemistry and Formation of the Beilby Layer During Polishing of Fused Silica Glass. Journal of the American Ceramic Society 98:2395–2402.
[tal21] Taleb, A., Shen, C., Mory, D. et al. (2021). Echelle spectrometer calibration by means of laser plasma. *Spectrochimica Acta Part B* 178:106144 1–13.
[tan03] Tanuma, S. and Kimura, T. (2003). Quantitative Auger and X-ray photoelectron analysis of Au-Cu alloys with three kinds of relative sensitivity factors. *Journal of Surface Analysis* 10: 163–168.
[tan09] Tantrakarn, K., Kato, N., Hokura, A., Nakai, I., Fujiib Y., and Gluščević, S. (2009). Archaeological analysis of Roman glass excavated from Zadar, Croatia, by a newly developed portable XRF spectrometer for glass. *X-Ray Spectrometry* 38:121–127.
[tre13] Trejos, T., Koons, R., Becker, S., Berman, T., Buscaglia, J.A., Duecking, M., Eckert-Lumsdon, T., Ernst, T., Hanlon, C., Heydon, A., Mooney, K., Nelson, R., Olsson, K., Palenik, C., Chip Pollock, E., Rudell, D., Ryland, S., Tarifa, A., Valadez, M., Weis, P., and Almirall, J. (2013). Cross-validation and evaluation of the performance of methods for the elemental analysis of forensic glass by μ-XRF, ICP-MS, and LA-ICP-MS. *Analytical and Bioanalytical Chemistry* 405(16):5393–5409.
[viv98] Vivien, C., Hermann, J., Perrone, A. et al. (1998). A study of molecule formation during laser ablation of graphite in low-pressure nitrogen. *Journal of Physics* 31:1263-1272.
[viv99] Vivien, C., Hermann, J., Perrone, A., and Boulmer-Leborgne, C. (1999). A study of molecule formation during laser ablation of graphite in low-pressure ammonia. *Journal of Physics D* 32:518-528.
[wid10] Widjonarko, N.E., Perkins, J.D., Leisch, J.E., Parilla, P.A., Curtis, C.J., Ginley, D.S., and Berry, J.J. (2010). Stoichiometric analysis of compositionally graded combinatorial amorphous thin film oxides using laser-induced breakdown spectroscopy. *Review of Scientific Instruments* 81:073103.
[yam11] Yamamoto, Y. and Yamamoto, K. (2011). Precise XPS depth profile of soda-lime-silica glass using C_{60} ion beam. Journal of Non-Crystalline Solids 356(1): 14–18
[yua10] Yuan, D. Q. and Xu, J. T. (2010). Quantitative analysis of ITO film by laser-induced breakdown spectroscopy. *Journal of Russian Laser Research* 31:350-356.
[yum02] Yun, J.-I., Klenze, R., and Kim, J.-I. (2002). Laser-induced breakdown spectroscopy for the on-line multielement analysis of highly radioactive glass melt simulants. Part II: analyses of molten glass samples. *Applied Spectroscopy* 56:852–858.
[yur89] Yurimoto, H., Kurosawa, M., and Sueno, S. (1989).Hydrogen analysis in quartz crystals and quartz glasses by secondary ion mass spectrometry. *Geochimica et Cosmochimica Acta* 53(3): 751–755.